

Tetragonal structure model for boehmite-derived γ -aluminaG. Paglia,¹ C. E. Buckley,^{1,*} A. L. Rohl,² B. A. Hunter,³ R. D. Hart,¹ J. V. Hanna,⁴ and L. T. Byrne⁵¹*Department of Applied Physics, Curtin University of Technology, Perth, WA, 6845, Australia*²*Department of Applied Chemistry, Curtin University of Technology, Perth, WA, 6845, Australia*³*Bragg Institute, Australian Nuclear Science and Technology Organisation, Sydney, NSW, 2234, Australia*⁴*ANSTO NMR Facility, Materials Division, Australian Nuclear Science and Technology Organisation, Sydney, NSW, 2234, Australia*⁵*NMR Facility, School of Biomedical and Chemical Sciences, University of Western Australia, Perth, WA, 6009, Australia*

(Received 10 March 2003; published 27 October 2003)

γ -alumina (γ -Al₂O₃) derived from boehmite has historically been described as having a cubic spinel structure with $Fd\bar{3}m$ symmetry, despite reports of tetragonal distortion in the structure. Based on neutron diffraction, transmission electron microscopy, and magic angle spinning NMR data, we propose a tetragonal model for the structure of boehmite-derived γ -Al₂O₃ with $I4_1/amd$ space group symmetry, a maximal subgroup of $Fd\bar{3}m$. It is also demonstrated that an accurate average structural model cannot be achieved if the cations are restricted to spinel positions.

DOI: 10.1103/PhysRevB.68.144110

PACS number(s): 61.66.-f, 61.12.-q, 61.14.-x

I. INTRODUCTION

γ -alumina (γ -Al₂O₃) is a transition alumina reported to occur at temperatures between 350 and 1000 °C.^{1,2} It is typically formed from an amorphous or boehmite precursor, and has remained present at temperatures as high as 1200 °C in the former case.³ Industrially, it is extremely important. It is used as a catalyst and catalyst support in the automotive and petroleum industries,⁴⁻⁷ in structural composites for spacecraft,⁸ miniature power supplies,^{9,10} and abrasive and thermal wear coatings.¹¹

Despite the industrial significance of γ -Al₂O₃, controversy still exists over its structure. A wide variety of experimental and computational methods have been used to describe the structure of γ -Al₂O₃ over the last half century. However, no definitive consensus has emerged on issues such as the arrangement of vacancies and the role of hydrogen in the structure. The mechanisms by which γ -Al₂O₃ behaves as a catalyst (or support) are not clearly understood. A clear understanding of the structure would aid in elucidating such mechanisms. The many variations of the structure reported are understandable as it has a high degree of disorder and small coherently scattering domain (CSD) sizes, resulting in diffuse diffraction patterns. There are also strong structural similarities with other transition aluminas, observed in the diffraction patterns, which can make it difficult to distinguish between phases in the same transformation sequence.

Initially γ -Al₂O₃ was reported as having a *cubic* spinel structure,¹² in accordance with the $Fm\bar{3}m$ space group, with a lattice parameter of 7.90 Å and Al sublattice occupations of 70% in octahedral site positions and 30% in tetrahedral site positions.^{13,14} It was later determined that this type of structure was more correctly described using the $Fd\bar{3}m$ space group, which is a maximal subgroup of the $Fm\bar{3}m$ group.^{15,16} The unit cell contains 32 oxygen ions in the Wyckoff 32*e* positions, which are approximately close packed in a face-centered-cubic (fcc) arrangement. The cation ratio in γ -Al₂O₃ is 2:3, as opposed to 3:4 for spinel structures, so to

maintain stoichiometry there must be $21\frac{1}{3}$ aluminum cations in the unit cell. This creates a defect spinel structure due to the vacancies imposed by such an arrangement. The consideration of a spinel structure restricts the aluminum cations to occupying the 8*a* (tetrahedral) and 16*d* (octahedral) Wyckoff positions, which are termed the *spinel* sites.

The greatest confusion surrounding γ -Al₂O₃ concerns the distribution of vacancies in the structure. Analysis of neutron diffraction, x-ray diffraction (XRD), and electron microscopy data has led various workers to conclude that the vacancies are situated either entirely in octahedral¹⁷⁻²⁰ or tetrahedral²¹⁻²³ sites, or distributed over both spinel sites.²⁴⁻²⁶ The ordering of the vacancies on octahedral sites is supported by several computational studies.²⁷⁻³¹ Vacancy ordering on tetrahedral sites is supported by a nuclear magnetic resonance spectroscopy³² (NMR) and a molecular dynamics³³ study. However, the NMR and computational work by Lee *et al.*³⁴ supports vacancy distribution among both octahedral and tetrahedral positions. Ushakov and Moroz³⁵ could not index XRD data with only spinel sites being occupied. A similar suggestion, for the occupation of more than just spinel sites, was made earlier for η -Al₂O₃, which has an analogous structure to γ -Al₂O₃.³⁶ Zhou and Snyder³⁷ reported cation occupation of a highly distorted Wyckoff 32*e* site, coinciding with reports of pentahedrally coordinated Al in several NMR studies^{26,38-40} and a molecular dynamics study.²⁷

When derived from amorphous precursors γ -Al₂O₃ has always been reported as having a cubic lattice.^{3,11,13,14,23,41-49} Boehmite-derived γ -Al₂O₃ has been reported as exhibiting a cubic lattice^{15,17,25,26,37,50,51} and as having a *tetragonal* distortion^{2,21,22,24,52-55} in the cubic lattice. Structural variations may result from varied preparation history.^{24,55-57} However, the most recent reports have either concluded or assumed in favor of a cubic lattice.^{25,26,37,51} There has also been a suggestion that γ -Al₂O₃ has two phases, both *cubic and tetragonal*.^{1,58}

The reports of tetragonal γ -Al₂O₃ found *c:a* ratios between 0.987 and 0.963.^{2,54} Yanagida and Yamaguchi⁵⁴ and

Wilson²⁴ found the degree of tetragonal distortion decreases with increasing preparation temperature. Wilson²⁴ also observed reduced tetragonal distortion with increased heating times. Tertian and Papee⁵² observed that rapid heating rates result in a cubic structure. Yanagida and Yamaguchi⁵⁴ performed *in situ* XRD followed by room temperature measurements and found that the tetragonal distortion was reduced at room temperature. The tetragonality has been attributed to shrinkage anisotropy in the *a* and *b* axes of boehmite during heating² and the distribution of residual water or hydroxyl ions.⁵⁴

The tetragonally distorted structure of γ -Al₂O₃ has continued to be ascribed to $Fd\bar{3}m$ symmetry.^{2,22} The tendency has been to simply assert a cubic structure and highlight a contracted *c* axis upon observation of a tetragonal distortion. This is not the crystallographically correct approach. Levin and Brandon⁵⁹ asserted that the *true* symmetry of the tetragonally deformed structures should be described by a tetragonal space group, expectedly, a maximal subgroup of $Fd\bar{3}m$.

It is well known that hydrogen is present at the surface of metal oxides; however, the role of hydrogen within the bulk structure of γ -Al₂O₃ is uncertain. This is an important topic because water is a by-product of the dehydration of boehmite. Several researchers since Dowden⁶⁰ have considered the presence of hydrogen, not bound in water form, within the bulk structure of γ -Al₂O₃. Proton NMR results from gel-derived alumina showed 0.009 g of hydrogen per gram of alumina within the structure, with 36.8% residing within the bulk.⁶¹ These passive protons have been suggested to account for the catalytic properties of the transition aluminas.^{4,62} de Boer and Houben⁶³ suggested a hydrogen-spinel (protospinel) structure for γ -Al₂O₃ analogous to the lithium spinel described by Kordes.⁶⁴ The protospinel approach is supported by several other researchers.^{35,65–67} As a result several researchers have proposed the stoichiometric formula for protospinel γ -Al₂O₃ be written γ -Al₂O₃ · *n*H₂O, with *n* reported to be between 0 and 0.63.^{35,37,61,63} This representation implies an excess of oxygen atoms and that γ -Al₂O₃ is a crystalline hydrate, which it is not.⁶⁷ Ushakov and Moroz³⁵ could only account for XRD data by incorporating residual hydrogen on nonspinel sites in the bulk structure. However, it should be noted that hydrogen cannot be distinctly seen by x rays. Hydrogen is better seen in bulk structures by neutrons, most suitably after deuterium exchange.⁶⁸ Tsyganenko *et al.*⁶⁵ attributed infrared spectra of O-H vibrations originating from the bulk to protons trapped in octahedral and tetrahedral vacancies within the anion lattice. This work is supported by the results of Saniger,⁶⁶ Wang *et al.*,²⁶ and Sohlberg *et al.*⁶⁷

Consideration of a protospinel structure may result in an idealized spinel structure, with no vacancies, represented by HAl₅O₈, or Al₂O₃ · 0.2H₂O. This is the same composition that was established for tohdite.⁶⁹ Sohlberg *et al.*⁶⁷ proposed an alternative stoichiometric notation for protospinel γ -Al₂O₃, H_{3*m*}Al_{2–*m*}O₃, where $m = 2n/(n + 3)$, which allows for a valid representation of the hydrogen content as opposed to the crystalline hydrate representation.

Contrary to the hydrogen-spinel-based structures reported,

Zhou and Snyder³⁷ found only small amounts of hydrogen in γ -Al₂O₃, one OH per unit cell. From this they specifically ruled out hydrogen spinel as a structural possibility. Their finding is supported by the theoretical calculations of Wolverton and Hass,³⁰ who found HAl₅O₈ to be thermodynamically unstable with respect to boehmite and decomposition to an anhydrous defect spinel. While Soled⁷⁰ has also provided alternative notation to represent γ -Al₂O₃, hydrogen was considered only to be prevalent at the surface with a considerable amount of amorphous content, most likely in the form of water, being implied. A series of molecular dynamics studies by Alvarez *et al.*^{27,71,72} supports postulations of a well-ordered, anhydrous, bulk structure with a defect-riddled surface containing many hydrogen species.

It should be noted that Zhou and Snyder³⁷ performed their analysis on γ -Al₂O₃ synthesized from highly crystalline boehmite, as in the current work. This is in contrast to studies that have concluded in favor of considerable quantities of hydrogen in the structure, such as Pearson⁶¹ and Wang *et al.*,²⁶ where gelatinous boehmite was the precursor. From this it becomes clear that the preparation route is important to consider.

When hydrogen content is considered the structure of γ -Al₂O₃ has been discussed using cubic symmetry.^{30,35,65,67,70} Cubic symmetry is also assumed for computer simulated studies of the bulk structure of γ -Al₂O₃, whether the presence of hydrogen is considered or not.^{27–31,34,67,71,73}

This paper assesses the bulk structural configuration of boehmite-derived γ -Al₂O₃ as part of ongoing research. In previous work, we investigated structural models for γ -Al₂O₃ from the literature and newly created models based on findings from NMR studies.⁷⁴ These models were shown to be inadequate for the boehmite-derived γ -Al₂O₃ data obtained by us due to discrepancies between the calculated diffraction peaks and the diffraction data, or due to failing the statistical Hamilton test.⁷⁵ This was particularly true for structural models that restricted Al to spinel positions. Neutron diffraction data contained what appeared to be split peaks, suggesting that the structure could be either tetragonal or consist of two phases, rather than cubic. This was confirmed by profile analysis.⁷⁴ The Zhou and Snyder³⁷ model (a cubic $Fd\bar{3}m$ representation of γ -Al₂O₃) provided the best fit of these models investigated at that time. Here a tetragonal model is developed that provides a better fit to extended experimental data and more accurately describes the structure of boehmite-derived γ -Al₂O₃. The issue of hydrogen in the bulk structure is also addressed.

II. EXPERIMENT

A. Materials

Powdered γ -Al₂O₃ was obtained from several highly crystalline boehmite precursors and used for neutron studies. Hydrogenated boehmite was obtained from the Alumina and Ceramics Laboratory, Malakoff Industries, Arkansas, USA. Deuterated boehmite was prepared by hydrothermal treatment of synthesized deuterated gibbsite with D₂O for 10

days at 158 °C in a Barc bomb. A further deuterated boehmite precursor was prepared by hydrothermal treatment of Alcoa C31 hydrogenated gibbsite with D₂O for 10 days at 158 °C in a Barc bomb. Each boehmite precursor was calcined at 600 °C, 7 hours for the deuterated samples and 13 hours for the hydrogenated sample. The calcined samples obtained were confirmed as γ -Al₂O₃ by matching its XRD pattern with ICDD pattern PDF 10-0425.

B. Neutron diffraction

Neutron diffraction data were collected *in situ* during calcination using the medium-resolution powder diffractometer (MRPD) at the High Flux Australian Reactor (HIFAR), operated by the Australian Nuclear Science and Technology Organization (ANSTO), Lucas Heights Laboratories, Sydney, Australia. Neutron diffraction data, using MRPD and the high-resolution powder diffractometer (HRPD) were also obtained at room temperature for hydrogenated boehmite, which had been precalcined to 600 °C for 7 hours.

C. Rietveld analysis and the starting structure models

Rietveld analysis^{76,77} of the neutron diffraction data from powdered γ -Al₂O₃ was performed using the LHPM Rietveld code with the Rietica 1.7.7 interface.⁷⁸ Four structural models were used in Rietveld refinements of the neutron diffraction data. The quality of the fit of the refined structure models to the data was determined by visual inspection of the difference plot and statistically by figures of merit of the estimated standard deviation of individual parameters. The figures of merit provided here are the profile factor (R_p), goodness of fit (χ^2), and Bragg factor (R_B), defined by Eqs. (1)–(3):⁷⁹

$$R_p = \frac{\sum |y_{io} - y_{ic}|}{\sum y_{io}}, \quad (1)$$

$$\chi^2 = \frac{\sum w_i (y_{io} - y_{ic})^2}{N - P}, \quad (2)$$

where w_i is the weight assigned to each observation, y_{io} and y_{ic} are the observed and calculated intensities at the i th step, respectively, N is the number of observations, and P is the number of least-squares parameters refined (these parameters provide an indication of the fit between the calculated diffraction pattern and the data), and

$$R_B = \frac{\sum |I_{ko} - I_{kc}|}{\sum I_{ko}}, \quad (3)$$

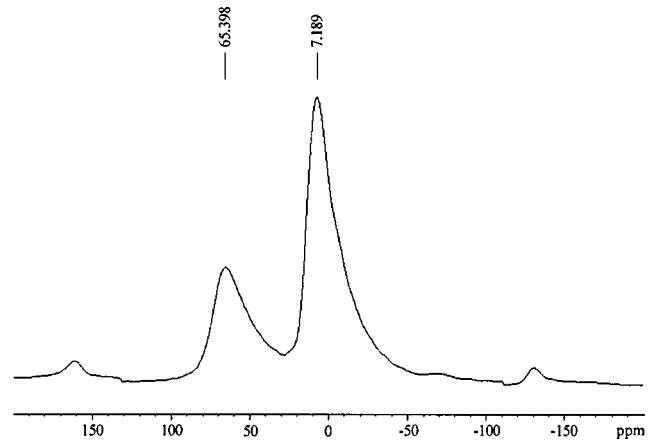


FIG. 1. MAS-NMR spectrum of γ -Al₂O₃ prepared from hydrogenated boehmite precursor; the octahedral peak is at 7.189 ppm and the tetrahedral peak is at 65.398 ppm.

where I_{ko} and I_{kc} are the observed and calculated intensities for Bragg reflection k , respectively. The Bragg factor represents how well a particular phase in the structural model fits to the data.

D. Nuclear magnetic resonance

A ²⁷Al magic angle spinning (MAS) NMR spectrum was recorded from the γ -Al₂O₃ calcination product of hydrogenated boehmite at ambient temperature using a Bruker MSL-400 spectrometer (9.4 T) operating at a ²⁷Al frequency of 104.23 MHz. The solid sample was spun around an axis inclined at 54°44' (the magic angle) with respect to the magnetic field, at an MAS rate of 15 kHz using a Bruker 4 mm double-air-bearing probe. The NMR spectrum was obtained after a 3 μ s 90, and a 0.6 μ s 90 pulse length on the solution and sample, respectively. A 1.0M Al(NO₃)₃ solution was employed as the chemical shift reference (set to 0.0 ppm), and for calibrating the experimental pulse lengths.

The baseline of the NMR spectrum was corrected before peak integration and peak deconvolution to obtain the coordination distribution of Al. This baseline correction was repeated 20 times to obtain an indication of its contribution to the uncertainty in the measurements.

E. Transmission electron microscopy

Dispersed samples of γ -Al₂O₃ on carbon film were investigated using a Philips 430 transmission electron microscope (TEM) fitted with a LaB₆ filament and operated at 300 kV. Selected area electron diffraction (SAED) patterns were obtained using a 660 mm camera length. The camera length was calibrated by comparison with diffraction patterns from pure gold. The absence of Kikuchi bands, attributable to the disorder in the structure, made it difficult to discern zone axes and thus difficult to obtain useful information using convergent beam electron diffraction (CBED).

III. RESULTS AND DISCUSSION

To date the best model describing the structure of γ -Al₂O₃ is that by Zhou and Snyder.³⁷ The key difference

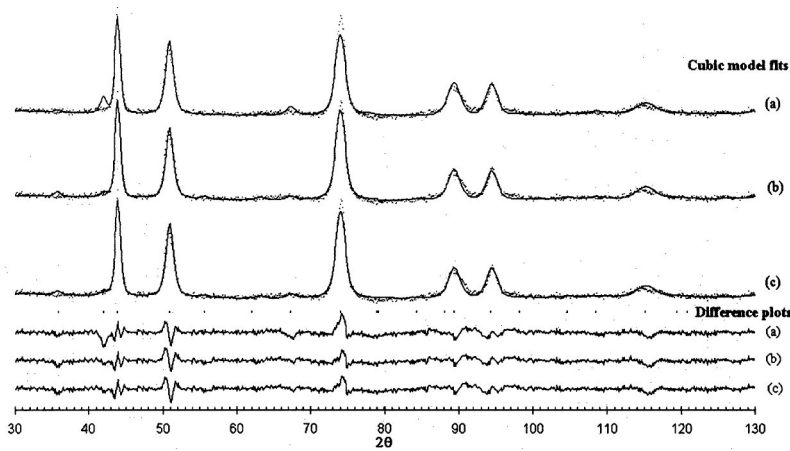


FIG. 2. Refinements for cubic models against neutron data obtained from deuterated boehmite heated *in situ* to form γ - Al_2O_3 ; (a) Cubic-1, incorporating only *spinel* site positions; (b) Zhou and Snyder (Ref. 37), (c) Cubic-16c. The solid lines in the diffraction patterns represent the calculated fit.

between the Zhou and Snyder³⁷ model and others is the incorporation of a *nonspinel* site position in the structural model, which follows from the work of Shirasuka *et al.*³⁶ and Ushakov and Moroz.³⁵ However, there are two discrepancies between the Zhou and Snyder³⁷ model and the data obtained here. The first relates to the report of the special Wyckoff 32*e* site position. The reported occupation of the highly distorted Wyckoff 32*e* site represents $\sim 25\%$ of the Al sublattice,³⁷ and $\sim 32\%$ when refined for the data analyzed here.⁷⁴ Only one NMR study of γ - Al_2O_3 derived from highly crystalline boehmite has reported pentahedrally coordinated Al, and this constituted no more than 6.5% of the Al sublattice.⁴⁰ The appearance of a peak representing *pentahedral* Al in such data can be debated. The occurrence of a “fivefold-coordinated peak” in NMR spectra of γ - Al_2O_3 is typically found for highly porous material made from poorly crystalline boehmite,^{26,80} or boehmitethat is well ground,³⁹ where higher surface areas result. From the literature it seems that the appearance of obvious pentahedral peaks in NMR spectra predominantly occurs for γ - Al_2O_3 where there is a high content of amorphous material, or when there is much surface cleavage resulting from milling.

The NMR spectrum (Fig. 1) obtained for the γ - Al_2O_3 sample examined herein shows two peaks, representing a cation sublattice with octahedral and tetrahedral coordination. There is no evidence of a fivefold-coordinated, or pentahedral, Al peak. What can only be said with certainty concerning this issue is that the asymmetric tailing of the peaks is indicative of short-range disorder in the structure.^{81–85} The spectrum is of similar appearance to those reported by Lee *et al.*³⁴ and Pecharroman *et al.*⁴⁰ Peak area integration of the data yields a distribution of 69(2)% octahedral and 31(2)% tetrahedral Al cation coordination, in excellent agreement with Lee *et al.*³⁴

Distorted octahedra, such as those described by Zhou and Snyder,³⁷ which may be regarded as pentahedral, have also been observed for κ - Al_2O_3 .^{86,87} This was the result of a slight distortion in the neighboring region of the oxygen sublattice. These distortions have not been found to result in a peak between the octahedral and tetrahedral peaks in the NMR spectra.⁸⁸ The greatest significance of the distorted octahedra in κ - Al_2O_3 is that the Al remains in an octahedral site position, which is consistent with the space group sym-

metry. In the $Fd\bar{3}m$ space group these can only be the 16*c* or 16*d* site positions. From crystallographic considerations, cleavage of the oxygen sublattice across an octahedra results in Al with a coordination number of five at a surface.⁸⁹ These cations, distorted or not, remain effectively in an octahedral position, which is more energetically favorable than the highly distorted 32*e* position. The proportion of Al in octahedral positions for the Zhou and Snyder³⁷ model is $\sim 44\%$, well below the quantity given by NMR studies. Added to the quantity of Al in the Wyckoff 32*e* site position, this yields a proportion of Al sublattice equivalent to $\sim 69\%$. Hence, we believe it is more appropriate to incorporate the 16*c* position for Al in the model as opposed to the 32*e*. This belief is supported by Wolverton and Hass,³⁰ who found some spontaneous nonspinel occupation on the 16*c* site for some of the theoretical structures they optimised.

Figure 2 illustrates the Rietveld refinements of the Zhou and Snyder³⁷ model and a cubic structural model incorporating the Wyckoff 16*c* site position in the Al sublattice, designated the Cubic-16*c* model. A cubic structural model with Al’s restricted to the spinel site positions, designated Cubic-1,⁷⁴ is also shown to illustrate the misfit between the calculated pattern and the data. The Zhou and Snyder³⁷ and Cubic-1 models were refined with background parameters incorporated rather than fixed.⁷⁴ When considering only spinel sites in the structural model, the vacancies were ordered on tetrahedral sites. In all other cases, the occupied site positions were all partially occupied. Table I displays the results of these refinements. The Zhou and Snyder³⁷ model, when refined here, yields an increase in the 32*e* occupancy at the expense of the 16*d* position and a slight change in the 32*e* position Al from $x=0.027$ to $x=0.019$. Refinement of the 32*e* position tended to make the refinement unstable, with its coordinates approaching either $x=0$ (the coordinates of the 16*c* position) or $x=0.25$ (the coordinates of the O sublattice). The refinement fits to the data of the Zhou and Snyder³⁷ and Cubic-16*c* models are very similar. However, the statistical indicators (Table I) indicate a slightly better fit for the latter model. Hence we conclude that the Cubic-16*c* model is equally as plausible as the Zhou and Snyder³⁷ model for representation of the average bulk structure of boehmite derived γ - Al_2O_3 .

TABLE I. Refinement results for cubic models against neutron data obtained from deuterated boehmite heated *in situ* to form γ -Al₂O₃. Uncertainties are to three standard deviations.

Model	Lattice parameters (Å)	Al site positions	Occupancy	R_p	Goodness of fit	Bragg factor
Cubic-1	$a=7.952(2)$	$8a$	0.83(1)	3.45	4.40	2.48
		$16d$	1.00(1)			
Zhou and Snyder ^a	$a=7.952(2)$	$8a$	0.83(2)	3.18	3.42	1.65
		$16d$	0.53(1)			
		$32e$	0.20(1)			
Cubic-16c	$a=7.953(2)$	$8a$	0.78(2)	3.07	3.16	1.35
		$16c$	0.34(1)			
		$16d$	0.60(1)			

^aReference 37.

Although the fits of the Zhou and Snyder³⁷ and Cubic-16c models are similar, the unit cell structures are considerably different. The 16c positions in the Cubic-16c structure are uniformly dispersed, whereas the Zhou and Snyder³⁷ model depicts a distribution of the 32e site positions in eight groups of four positions uniformly throughout the unit cell. The Al atoms are distributed isotropically among these sites. Each group of four 32e positions closely surrounds an oxygen atom. The close proximity of these sites to the neighboring oxygen, and each other, suggests that it is only possible for one Al ion to be present among a group of four 32e positions, which yields a maximum possible occupancy of 0.25 Al's in this site position.

The second discrepancy between the Zhou and Snyder³⁷ model and the data examined here more specifically relates to the consideration of a cubic space group in general. All of the peaks in the diffraction pattern, with the exception of the peak at $2\theta \sim 44^\circ$, appear to be split. This was observed for all the neutron diffraction patterns collected from every sample. This splitting is most obvious for the peak at $2\theta \sim 51^\circ$ (see Fig. 3). Profile analysis shows a much better goodness-of-fit when multiple peaks are considered as opposed to one peak.⁷⁴ The appearance of these split peaks, exhibiting an improved profile when considering two or more peaks, is characteristic of a structure of lower symmetry than cubic, such as a *tetragonal* structure. Rietveld refinement of both tetragonal and dual-phase structure models (discussed later) provides better profile fits to the peaks than the cubic models (Fig. 3).

A. Space group identification from TEM

A systematic TEM examination revealed a granular morphology consisting of layered triangular and rhombohedral-like plates, consistent with previous observations.^{2,22} Selected area electron diffraction of individual plates showed only one type of pattern, indicative of a single-phase material. The diffraction patterns observed are depicted in Fig. 4. Figure 4(a), imaged from the plate surface, is consistent with the diffraction patterns observed by Lippens and de Boer² and Saalfeld and Mehrotra.²² Lippens and de Boer² observed that the electron diffraction patterns of boehmite-derived γ -Al₂O₃ contained more spots than expected from the spinel structure and a contracted *c* lattice parameter. Irrespective of the obvious tetragonal nature of boehmite-derived γ -Al₂O₃, researchers have continued to index the structure in accordance with the $Fd\bar{3}m$ space group. The *tetragonal* $I4_1/amd$ space group is a maximal subgroup of $Fd\bar{3}m$, with $a_{\text{cubic}} \approx \sqrt{2}a_{\text{tetragonal}}$. These patterns can be described by $I4_1/amd$ symmetry as opposed to $Fd\bar{3}m$ (Fig. 4). In the $I4_1/amd$ representation the *a* parameter is equivalent to d_{110} (~ 5.62 Å) in the cubic representation. Using this representation the data yield $a \sim 5.60$ Å and $c \sim 7.83$ Å, which is consistent with the Rietveld data. Indexing by $I4_1/amd$ symmetry satisfies the reflection conditions of the space group¹⁶ and remains consistent with the three types of reflections described by Lippens and de Boer.² The significance of the types of reflections observed have been discussed previously.^{2,22,24} A conversion table from reflections based on $Fd\bar{3}m$ to $I4_1/amd$ symmetry is provided in Table II.

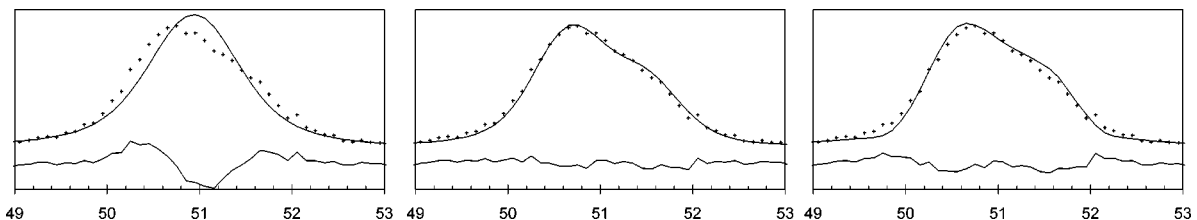


FIG. 3. Resulting profiles of the peak at $2\theta \sim 51^\circ$ generated by refinement of structure models; (a) cubic, based on the Zhou and Snyder (Ref. 37) and Cubic-16c models, (b) tetragonal, based on the model designated Tetragonal-8c, (c) dual phase, based on Cubic-16c combined with Tetragonal-8c models.

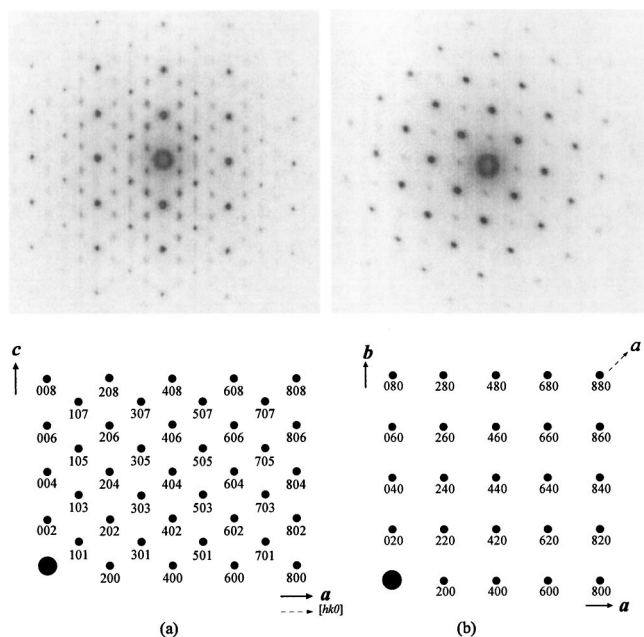


FIG. 4. TEM diffraction patterns, with tetragonal, $I4_1/amd$, indexing diagrams below, looking down the (a) $[0k0]$ and (b) $[00l]$ zone axes. Dashed lines indicate the axis if the traditional cubic representation were followed.

B. Proposed tetragonal model

$I4_1/amd$ symmetry was first suggested by Li *et al.*,¹⁹ who proposed a structure with Al restricted to spinel sites and vacancy ordering on octahedral sites. In this space group the site positions analogous to the spinel sites in its supergroup are the $4a$ ($\equiv 8a$) and $8d$ ($\equiv 16d$) sites.¹⁶ This space group was utilized in a new structural model for Rietveld analysis, adopting the same approach as Cubic- $16c$, and designated Tetragonal- $8c$. The resulting unit cell has 16 oxygen ions, on the $16h$ site position, and $10\frac{2}{3}$ aluminum cations to maintain 2:3 stoichiometry. The starting occupancies used for the Tetragonal- $8c$ model were those resulting from the refinement of the Cubic- $16c$ model. Results of the refinements of this model are summarized in Tables III and IV, with an example of the fit illustrated in Fig. 5. In every case a significantly better fit resulted for the Tetragonal- $8c$ model than for any of the cubic models examined. Table III illustrates consistency of the model data for all specimens examined, with the spread in the occupancy no greater than 0.04 between all samples. The distribution of the Al ions between octahedral and tetrahedral positions agrees with the NMR data in every case. Consistency of the model also pervaded through the interatomic distances, which showed a deviation no larger than 0.1 Å for any equivalent distance between all samples.

For all models examined, the Al ions were linked while they were refined to maintain the 2:3 ratio required by the formula Al_2O_3 . However, to test the stability of the Tetragonal- $8c$ model, the Al ions were also refined unlinked. Individual occupancies deviated less than 0.5% from their linked counterparts and the overall stoichiometry remained

within 1% of the ideal 2:3 ratio for alumina. A summary of the structure is presented in Table IV.

The consistency of the structural model between *in situ* heating and room temperature data strengthens the argument against a special pentahedral Al. It is also indicative of the stability of the phase at both ambient and calcination temperatures. The disorder evident in the NMR data indicates that a good fit to the diffraction data can be difficult to achieve. However, the structural model accounts for this by using larger thermal parameters than seen in a more ordered structure such as α -alumina.

A dual-phase model was also refined against the data. This approach was first suggested by Gan^{1,58} and investigated previously.⁷⁴ Here, the Tetragonal- $8c$ and Cubic- $16c$ models were combined to form the dual-phase model. Although the refinement was successful as opposed to previous attempts^{58,74} the figures of merit were higher than for any single-phase Tetragonal- $8c$ refinement, with a profile factor of 2.79, a goodness of fit of 2.39, and Bragg factors of 1.89 and 0.56 for the tetragonal and cubic phases, respectively. This is in spite of the greater number of parameters refined for the dual-phase model, which usually result in better figures of merit. The dual-phase refinement also demonstrated unrealistic instability in site occupancy parameters due to high correlation between the phases. Based on these results and the observations from TEM, a dual-phase model is discounted for the boehmite-derived γ - Al_2O_3 examined here. Consistency of the Tetragonal- $8c$ model for all data sets strengthens the argument for one phase as opposed to two phases.

C. Consideration of hydrogen

From the literature it appears that the occurrence of hydrogen within the bulk structure is dependent on the precursor material used. For all the refinements attempted above there remains some differences between the data and the calculated pattern, particularly at $2\theta \sim 44^\circ$. This difference also remains in the refinement determined by Zhou and Snyder.³⁷ This is the peak that draws the greatest intensity contribution from the oxygen sublattice. From suggestions in the literature that there is some hydroxyl substitution for oxygen in the bulk structure,^{26,65} it was decided to consider hydrogen in Rietveld refinements to investigate if this would account for the intensity mismatch at $2\theta \sim 44^\circ$. This was done by measuring the amount of hydrogen in the samples and incorporating this amount as deuterium in refinements of deuterated samples. Deuterated samples were used for the refinements instead of hydrogenated samples due to the high incoherent background caused by hydrogen. In the following discussion concerning the Rietveld refinements the word hydrogen is used instead of deuterium for clarity.

To determine the amount of hydrogen in the sample examined here, one-shot ignition loss was performed on the hydrogenated γ - Al_2O_3 sample. For the ignition loss the sample was initially heated to 200 °C for 2 hours to drive off surface-adsorbed water and cooled in a desiccator. The sample was then weighed to ± 1 mg precision, heated to 1200 °C for 1 hour to drive off all residual hydroxyl ions from the bulk, cooled, and weighed again. From this proce-

TABLE II. Equivalent Miller indices for the cubic and tetragonal, $I4_1/amd$, representations of the structure of $\gamma\text{-Al}_2\text{O}_3$.

From Fig. 4(a): $[0k0]$ zone axis		From Fig. 4(b): $[00l]$ zone axis	
Cubic	Tetragonal	Cubic	Tetragonal
hkl	hkl	hkl	hkl
0 0 4	0 0 4	2 -2 0	0 2 0
0 0 8	0 0 8	2 2 0	2 0 0
0 0 12	0 0 12	4 0 0	2 2 0
1 1 1	1 0 1	4 -4 0	0 4 0
1 1 3	1 0 3	4 4 0	4 0 0
1 1 5	1 0 5	6 -6 0	0 6 0
1 1 7	1 0 7	6 -2 0	2 4 0
2 2 0	2 0 0	6 2 0	4 2 0
2 2 2	2 0 2	6 6 0	6 0 0
2 2 4	2 0 4	8 -8 0	0 8 0
2 2 6	2 0 6	8 -4 0	2 6 0
2 2 8	2 0 8	8 0 0	4 4 0
3 3 1	3 0 1	8 8 0	8 0 0
3 3 3	3 0 3	8 4 0	6 2 0
3 3 5	3 0 5	10 -6 0	2 8 0
3 3 7	3 0 7	10 -2 0	4 6 0
4 4 0	4 0 0	10 2 0	6 4 0
4 4 2	4 0 2	10 6 0	8 2 0
4 4 4	4 0 4	12 -4 0	4 8 0
4 4 6	4 0 6	12 4 0	8 4 0
4 4 8	4 0 8	12 0 0	6 6 0
5 5 1	5 0 1	14 -2 0	6 8 0
5 5 3	5 0 3	14 2 0	8 6 0
5 5 5	5 0 5	16 0 0	8 8 0
5 5 7	5 0 7		
6 6 0	6 0 0		
6 6 2	6 0 2		
6 6 4	6 0 4		
6 6 6	6 0 6		
6 6 8	6 0 8		
7 7 1	7 0 1		
7 7 3	7 0 3		
7 7 5	7 0 5		
7 7 7	7 0 7		
8 8 0	8 0 0		
8 8 2	8 0 2		
8 8 4	8 0 4		
8 8 6	8 0 6		
8 8 8	8 0 8		

ture the residual amount of hydrogen species in the bulk was determined to be 2.26(3) wt %. This is assumed to be in the form of water from the decomposition reaction of boehmite.⁵⁷ From the ignition loss $n=0.131(2)$, giving the traditional protospinel stoichiometry as $\gamma\text{-Al}_2\text{O}_3 \cdot 0.131\text{H}_2\text{O}$, which equates to 1.39(8) hydrogens per tetragonal unit cell. The treatment of Sohlberg *et al.*⁶⁷ gives $\text{H}_{0.251}\text{Al}_{1.916}\text{O}_3$.

The incorporation of the measured amount of hydrogen in the sample via Rietveld refinement followed two approaches,

designated approach 1 and approach 2. Approach 1 involved sampling the hydrogen in various interstitial octahedral and tetrahedral positions, consistent with space group symmetry, following from the findings of Tsyganenko *et al.*⁶⁵ and Sohlberg *et al.*⁶⁷ Approach 2 was more generic; the hydrogen was given starting coordinates which placed it at a physically reasonable distance from oxygen, using the same symmetry position used for oxygen. These two procedures were systematically employed for all structural models tested, which included the cubic and tetragonal models with Al's restricted to spinel site positions, in addition to those where Al's were refined on nonspinel site positions.

The Rietveld refinements carried out for approaches 1 and 2 were conducted under two further conditions. The first was to maintain Al_2O_3 stoichiometry and incorporate the hydrogen as additional material within the bulk, consistent with $\gamma\text{-Al}_2\text{O}_3 \cdot n\text{H}_2\text{O}$ representation. The second was to incorporate the hydrogen according to the resulting stoichiometry of the Sohlberg *et al.*⁶⁷ representation.

For refinements where Al_2O_3 stoichiometry was maintained, refinements were more favorable when using approach 2. Sustaining a stable refinement was extremely difficult when the occupancy of hydrogen was fixed to physically reasonable values for approach 1. When catastrophic divergence in the refinement was avoided the resulting fit was poor with high figures of merit relative to any of those obtained from the corresponding models that did not incorporate hydrogen (the anhydrous models). When the occupancy of hydrogen was refined, negative values always resulted, indicating that the hydrogen did not prefer any of the assigned interstitial occupations. Unstable thermal parameters also resulted.

This was not the case for approach 2. Refinements were stable for hydrogen occupancy fixed to physically reasonable values. Moreover, hydrogen occupancy generally remained physically reasonable when allowed to refine. Only in some cases did the hydrogen occupancy tend to become unreasonably large. The thermal parameters tended to become either uncharacteristically large, suggesting considerable migration of hydrogen through the structure, or negatively unstable. In all cases, the best results were obtained when the hydrogen was incorporated in the Tetragonal-8c model, as opposed to any other tetragonal, cubic, or dual-phase model. The best stable refinement yielded a profile factor of 2.75, a goodness of fit of 2.50, and a Bragg factor of 2.42.

Refining using the stoichiometry implied by the Sohlberg *et al.*⁶⁷ representation also resulted in the best fits being obtained for incorporation of hydrogen in the Tetragonal-8c model. Maintaining $\text{Al}_{1.916}\text{O}_3$ stoichiometry results in 10.21 Al's in the unit cell as opposed to $10\frac{2}{3}$, to allow for the residual hydrogen. The same trends in instabilities, including the greater success in refining using approach 2 were observed, as per the refinements where Al_2O_3 stoichiometry was maintained. When the parameters were maintained within physically reasonable limits the best stable refinement yielded a profile factor of 2.68, a goodness of fit of 2.32, and a Bragg factor of 2.04. These results suggest that the

TABLE III. Refinement results for the Tetragonal-8c model of γ -Al₂O₃ from the various precursors: 1, deuterated boehmite prepared hydrothermally from deuterated gibbsite and calcined *in situ*; 2, deuterated boehmite prepared hydrothermally from hydrogenated gibbsite and calcined *in situ*; 3, hydrogenated boehmite calcined *in situ*; 4, precalcined hydrogenated boehmite with data collected at room temperature. All refinements were made for MRPD data except where indicated. Uncertainties are to three estimated standard deviations.

Precursor	Lattice Parameters (Å)	Al site positions	Occupancy	R_p	χ^2	R_B
1	$a = 5.652(1)$	4a	0.78(2)	2.47	1.96	0.99
	$c = 7.871(5)$	8c	0.36(1)			
		8d	0.58(1)			
2	$a = 5.660(2)$	4a	0.78(2)	3.12	2.59	0.90
	$c = 7.866(5)$	8c	0.35(1)			
		8d	0.59(1)			
3	$a = 5.639(2)$	4a	0.77(2)	2.94	2.25	0.97
	$c = 7.867(2)$	8c	0.36(1)			
		8d	0.58(1)			
4	$a = 5.616(3)$	4a	0.75(2)	3.08	2.06	1.28
	$c = 7.836(6)$	8c	0.37(1)			
		8d	0.59(1)			
4 (HRPD)	$a = 5.615(2)$	4a	0.79(2)	3.35	1.73	1.34
	$c = 7.835(4)$	8c	0.35(1)			
		8d	0.59(1)			

protospinel representation of Sohlberg *et al.*⁶⁷ is more appropriate than the traditional γ -Al₂O₃·*n*H₂O representation.

The figures-of-merit of the best protospinel refinements for the γ -Al₂O₃ examined here show fits that are not as good as those obtained for either the anhydrous Tetragonal-8c (Table IV.) model or the Zhou and Snyder³⁷ and Cubic-16c models. In addition there were significant residual differences between calculated peaks and the data. These were reflected in poor profile fits when compared to the anhydrous Tetragonal-8c model and, in some cases, additional calculated peaks were present with none corresponding to the

data. It was also found that none of the tested protospinel models improved the calculated to data intensity mismatch at $2\theta \sim 44^\circ$.

To further test the stability of the most successful protospinel refinement models tested for the present data, they were allowed to refine with the Al ions unlinked, as per the anhydrous Tetragonal-8c model. This improved the visual appearance of the peaks but at the expense of the crystallographic integrity of the models. In cases where the Al ions were restricted to spinel positions the overall stoichiometry deviated up to 40% below the ideal stoichiometry. For

TABLE IV. Structural parameters of boehmite derived γ -Al₂O₃ for space group $I4_1/amd$, $a = 5.652(1)$, $c = 7.871(5)$, $R_p = 2.47$, $\chi^2 = 1.96$, $R_B = 0.99$. Data taken from the refinement of neutron data of deuterated boehmite prepared hydrothermally from deuterated gibbsite and calcined *in situ*. Uncertainties are to three standard deviations.

Site	x	y	z	B (Å ²)	Occupancy
O (16h)	0	0.0076(30)	0.2516(40)	1.4(3)	1.0
Al (4a)	0	0.75	0.125	2.2(3)	0.78(2)
Al (8c)	0	0	0	2.3(3)	0.36(1)
Al (8d)	0	0	0.5	2.3(3)	0.58(1)
Core geometries (distances in Å, angles in deg) around Al ions					
Al (4a)-O	1.764(33)				
Al (8c)-O	1.981(33)	2.029(18)			
Al (8d)-O	1.956(32)	1.968(18)			
O-Al(4a)-O	111.23(1.47)	108.60(72)			
O-Al(8c)-O	180.00	91.22(1.26)	88.78(1.26)		
O-Al(8d)-O	180.00	91.27(1.35)	88.73(1.35)		

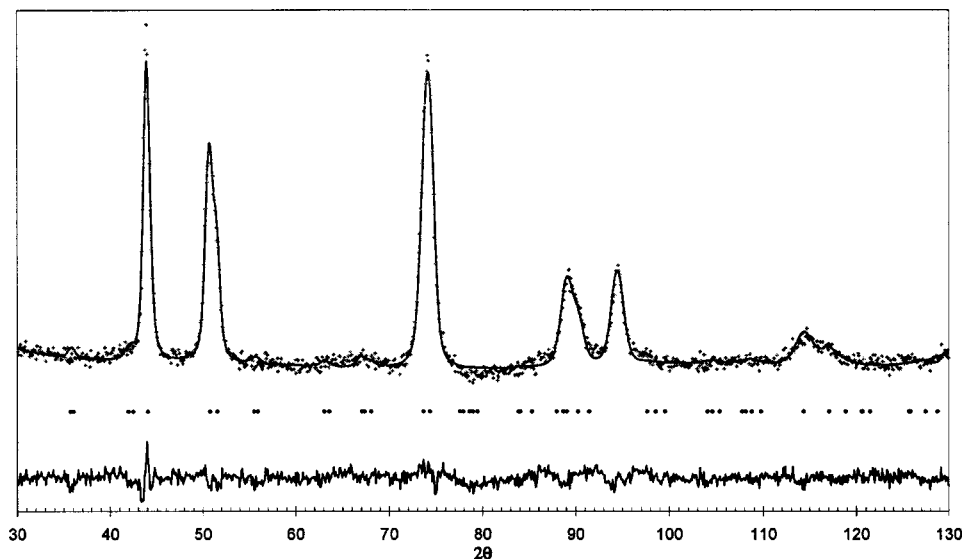


FIG. 5. Rietveld refinement of the Tetragonal-8c model for γ -Al₂O₃ prepared by heating *in situ* from deuterated boehmite precursors.

nonspinel site Al occupation in the protospinel models, the deviation from ideal stoichiometry was up to 30%. This is in distinct contrast to the anhydrous Tetragonal-8c model tested above.

The results from the protospinel trials suggest that there is no interstitial hydrogen within the crystalline bulk structure of the boehmite-derived γ -Al₂O₃ examined here. Its presence appears to be limited to the surface, as expected, and in the form of water within the amorphous content of the material. Prompt gamma activation analysis⁹⁰⁻⁹² (PGAA) and inelastic neutron scattering⁹³ (INS) is being conducted to further investigate the presence of water and hydroxide groups within the structure.⁹⁴

IV. CONCLUSIONS

Boehmite-derived γ -Al₂O₃, where a tetragonal distortion is observed, is best described using the $I4_1/amd$ space group rather than $Fd\bar{3}m$. This is evident from peak splitting in neutron powder diffraction data and from TEM. The structure could not be accurately modeled by restricting the Al ions to spinel positions. As a result, occupation of the 8c Wyckoff position in addition to the 4a and 8d is proposed. No evidence of fivefold-coordinated Al atoms within the structure was found in the NMR data obtained in this study. This and the subsequent Rietveld analysis suggest that the Al ions can only be situated in octahedral or tetrahedral positions. The Tetragonal-8c model (Table IV) accommodates the observed peak splitting better than all other models investigated. The distribution of Al ions determined from the proposed Tetragonal-8c structural model is in agreement with the distribution obtained from NMR data. Consistency

of this model for all data sets strengthens the argument for one phase as opposed to two phases. In this model there is ordering of vacancies on all the site positions, tetrahedral and octahedral. From this we can see why ambiguity has arisen in early work as to which sites the vacancies prefer to reside in. It also appears that, for the material examined here, hydrogen is not interstitially present within the crystalline bulk structure, but rather is in the form of water, within the amorphous content. There still remains some differences between the data and the calculated pattern, particularly at $2\theta \sim 44^\circ$, which, to date, no model has been able to accommodate. We hope to elucidate this by computer simulations in the future.

ACKNOWLEDGMENTS

G.P. would like to thank the Australian government for financial support to fund this research. G.P. is also grateful to the Australian Institute of Nuclear Science and Engineering (AINSE) for the provision of access to the facilities at ANSTO and additional support from AINSE. Thanks also to the Western Australian Interactive Virtual Environments Center (IVEC) for provision of further support. Gratitude is also extended to Dr. Margaret Elcombe and Dr. Andrew Studer, of ANSTO, who provided valuable assistance and advice for the research project. Special thanks go to Professor Brian O'Connor and Karsten Winter, of Curtin University of Technology, Professor Robert Snyder, of the Georgia Institute of Technology, Atlanta, USA, and Dr. Terry Udovic of the National Institute of Standards and Technology (NIST), Gaithersburg, USA, who provided very useful advice. G.P. would also like to thank Professor Andrew Johnson, University of Western Australia, for assistance he gave.

*Corresponding author. Email address: c.buckley@exchange.curtin.edu.au

¹B. O'Connor, D. Li, B.K. Gan, B. Latella, and J. Carter, *Adv. X-Ray Anal.* **41**, 659 (1999).

²B.C. Lippens and J.H. de Boer, *Acta Crystallogr.* **17**, 1312 (1964).

³T.C. Chou and T.G. Nieh, *J. Am. Ceram. Soc.* **74**, 2270 (1991).

⁴S.E. Tung and E. Mcininch, *J. Catal.* **3**, 229 (1964).

⁵H. Knözinger and P. Ratnasamy, *Catal. Rev.-Sci. Eng.* **17**, 31 (1978).

⁶K. Taylor, in *Catalysis: Science and Technology*, edited by J.R. Anderson and M. Moudart (Springer-Verlag, Berlin, 1984), p. 119.

- ⁷B.C. Gates, Chem. Rev. (Washington, D.C.) **95**, 511 (1995).
- ⁸G.G. Rosanova, 12th Annual AIAA/USU Conference on Small Satellites, Logan, Utah, 1998.
- ⁹M.K. Drost, C.J. Call, J.M. Cuta, and R.S. Wegeng, Microscale Thermophys. Eng. **1**, 321 (1997).
- ¹⁰P.B. Koeneman, I.J. Busch-Vishniac, and K.L. Wood, J. Microelectromech. Syst. **6**, 355 (1997).
- ¹¹R. McPherson, J. Mater. Sci. **15**, 3141 (1980).
- ¹²K.E. Sickafus, J.M. Wills, and N.W. Grimes, J. Am. Ceram. Soc. **82**, 3279 (1999).
- ¹³E.J.W. Verwey, Z. Kristallogr. **91**, 65 (1935a).
- ¹⁴E.J.W. Verwey, Z. Kristallogr. **91**, 317 (1935b).
- ¹⁵H.B. Rooksby, in *X-ray Identification and Crystal Structures of Clay Minerals*, edited by G.W. Brindley (Mineralogical Society, London, 1951), Chap. 10.
- ¹⁶*International Tables of Crystallography*, edited by T. Hahn (Kluwer, London, 1995), Vol. A.
- ¹⁷K.P. Sinha and A.P.B. Sinha, J. Phys. Chem. **61**, 758 (1957).
- ¹⁸H. Jagodzinski and H. Saalfeld, Z. Kristallogr. **110**, 197 (1958).
- ¹⁹D.Y. Li, B.H. O'Conner, G.I.D. Roach, and J.B. Cornell, XVth Congress of the International Union of Crystallography (Bordeaux, 1990), Abstracts volume C.
- ²⁰G.N. Kryukova, D.O. Klenov, A.S. Ivanova, and S.V. Tsybulya, J. Eur. Ceram. Soc. **20**, 1187 (2000).
- ²¹H. Saalfeld, Clay Miner. Bull. **3**, 249 (1958).
- ²²H. Saalfeld and B. Mehrotra, Ber. Dtsch. Keram. Ges. **42**, 161 (1965).
- ²³V. Jayaram and C.G. Levi, Acta Metall. **37**, 569 (1989).
- ²⁴S.J. Wilson, Solid State Chem. **30**, 247 (1979).
- ²⁵Y.G. Wang, P.M. Bronsveld, and J.T.M. DeHosson, J. Am. Ceram. Soc. **81**, 1655 (1998).
- ²⁶J.A. Wang, X. Bokhimi, A. Morales, O. Novaro, T. Lopez, and R. Gomez, J. Phys. Chem. B **103**, 299 (1999).
- ²⁷L.J. Álvarez, J.F. Sanz, M.J. Capitán, and J.A. Odriozola, Chem. Phys. Lett. **192**, 463 (1992).
- ²⁸S.-D. Mo, Y.-N. Xu, and W.-Y. Ching, J. Am. Ceram. Soc. **80**, 1193 (1997).
- ²⁹F.H. Streitz and J.W. Mintmire, Phys. Rev. B **60**, 773 (1999).
- ³⁰C. Wolverton and K.C. Hass, Phys. Rev. B **63**, 024102 (2001).
- ³¹G. Gutiérrez, A. Taga, and B. Johansson, Phys. Rev. B **65**, 012201 (2002).
- ³²C.S. John, N.C.M. Alma, and G.R. Hays, Appl. Catal. **6**, 341 (1983).
- ³³S. Blonski and S.H. Garofalini, Surf. Sci. **195**, 263 (1993).
- ³⁴M.-H. Lee, C.-F. Cheng, V. Heine, and J. Klinowski, Chem. Phys. Lett. **265**, 673 (1997).
- ³⁵V.A. Ushakov and E.M. Moroz, React. Kinet. Catal. Lett. **24**, 113 (1984).
- ³⁶K. Shirasuka, H. Yanagida, and G. Yamaguchi, Yogyo Kyokaishi **84**, 610 (1976).
- ³⁷R.-S. Zhou and R.L. Snyder, Acta Crystallogr., Sect. B: Struct. Sci. **B47**, 617 (1991).
- ³⁸R. Dupree, M.H. Lewis, and M.E. Smith, Philos. Mag. A **53**, L17 (1986).
- ³⁹F.R. Chen, J.G. Davis, and J.J. Fripiat, J. Catal. **133**, 263 (1992).
- ⁴⁰C. Pecharroman, I. Sobrados, J.E. Iglesias, T. Gonzales-Carreno, and J. Sanz, J. Phys. Chem. B **103**, 6160 (1999).
- ⁴¹M. Plummer, J. Appl. Chem. **8**, 35 (1958).
- ⁴²J. Harvey, H.I. Mathews, and H. Wilman, Discuss. Faraday Soc. **30**, 113 (1960).
- ⁴³A.L. Dragoo and J.J. Diamond, J. Am. Ceram. Soc. **50**, 568 (1967).
- ⁴⁴R. McPherson, J. Mater. Sci. **8**, 851 (1973).
- ⁴⁵F.W. Dynys and J.W. Halloran, J. Am. Chem. Soc. **65**, 442 (1982).
- ⁴⁶K.J. Morrissey, K.K. Czanderna, R.P. Merrill, and C.B. Carter, Ultramicroscopy **18**, 379 (1985).
- ⁴⁷J.E. Bonevich and L.D. Marks, J. Mater. Res. **7**, 1489 (1992).
- ⁴⁸B. Ealet, M.H. Elyakhloufi, E. Gillet, and M. Ricci, Thin Solid Films **250**, 92 (1994).
- ⁴⁹I. Levin, D.G. Bendersky, D.G. Brandon, and M. Ruhle, Acta Metall. **45**, 3659 (1997).
- ⁵⁰H.C. Stumpf, A.S. Russell, J.W. Newsome, and C.M. Tucker, Ind. Eng. Chem. **42**, 1398 (1950).
- ⁵¹K. Liddell, PDF 50-0741, JCPDS Database (1996).
- ⁵²R. Tertian and D. Papee, J. Chim. Phys. Phys.-Chim. Biol. **55**, 341 (1958).
- ⁵³H. Yanagida and G. Yamaguchi, Bull. Mater. Sci. **35**, 1896 (1962).
- ⁵⁴H. Yanagida and G. Yamaguchi, Bull. Chem. Soc. Jpn. **37**, 1229 (1964).
- ⁵⁵S.J. Wilson and J.D.C. McConnell, J. Solid State Chem. **34**, 315 (1980).
- ⁵⁶T. Tsuchida, R. Furuichi, and T. Ishii, Thermochim. Acta **39**, 103 (1980).
- ⁵⁷K. Wefers and C. Misra, *Oxides and Hydroxides of Aluminum*, Technical Paper No. 19 (Alcoa Laboratories, Pittsburgh, 1987).
- ⁵⁸B.K. Gan, Ph. D. thesis, School of Physical Sciences, Curtin University of Technology, Perth, Australia, 1996).
- ⁵⁹I. Levin and D. Brandon, J. Am. Ceram. Soc. **81**, 1995 (1998).
- ⁶⁰D.A. Dowden, J. Chem. Soc. **1-2**, 242 (1950).
- ⁶¹R.M. Pearson, J. Catal. **23**, 388 (1971).
- ⁶²A.A. Tsyganenko and P.P. Mardilovich, J. Chem. Soc., Faraday Trans. **92**, 4843 (1996).
- ⁶³J.H. de Boer and G.M.M. Houben, Proceedings of the International Symposium on the Reactivity of Solids (Flanders Boktryckeri Aktiebolag, Göteborg), **1**, 237 (1952).
- ⁶⁴E. Kordes, Z. Kristallogr. **91**, 202 (1935).
- ⁶⁵A.A. Tsyganenko, K.S.S. Mirnov, A.M. Rzhetskij, and P.P. Mardilovich, Mater. Chem. Phys. **26**, 35 (1990).
- ⁶⁶J.M. Saniger, Mater. Lett. **22**, 109 (1995).
- ⁶⁷K. Sohlberg, S.J. Pennycook, and S.T. Pantelides, J. Am. Ceram. Soc. **121**, 7493 (1999).
- ⁶⁸C.J. Howard and S.J. Kennedy, Mater. Forum **18**, 155 (1994).
- ⁶⁹G. Yamaguchi, H. Yanagida, and S. Ono, Bull. Chem. Soc. Jpn. **37**, 752 (1964).
- ⁷⁰S. Soled, J. Catal. **81**, (1983).
- ⁷¹L.J. Álvarez, L.E. León, J.F. Sanz, M.J. Capitán, and J.A. Odriozola, J. Phys. Chem. **99**, 17 872 (1995).
- ⁷²L.J. Álvarez, J.F. Sanz, M.J. Capitán, M.A. Centeno, and J.A. Odriozola, Chem. Soc., Faraday Trans. **89**, 3623 (1993).
- ⁷³G.W. Watson and D.J. Willock, Chem. Commun. (Cambridge) **12**, 1076 (2001).
- ⁷⁴G. Paglia, C.E. Buckley, A.L. Rohl, and L.T. Byrne, J. Australas. Ceram. Soc. **38**, 92 (2002).
- ⁷⁵C. Giacomazzo, in *Fundamentals of Crystallography*, edited by

- C. Giacobozzo (Oxford Scientific Publications, Oxford, 1992), p. 103.
- ⁷⁶H.M. Rietveld, *J. Appl. Crystallogr.* **2**, 65 (1969).
- ⁷⁷*The Rietveld Method*, edited by R.A. Young, International Union of Crystallography (Oxford University Press, New York, 1993).
- ⁷⁸B.A. Hunter, IUCr Commission on Powder Diffraction Newsletter **20**, article 16 (1998).
- ⁷⁹R.A. Young and D.B. Wiles, *J. Appl. Crystallogr.* **15**, 430 (1982).
- ⁸⁰S. Komarneni, R. Roy, C.A. Fyfe, and G.J. Kennedy, *J. Am. Ceram. Soc.* **68**, C243 (1985).
- ⁸¹B.L. Phillips, R.J. Kirkpatrick, and G.L. Hovis, *Phys. Chem. Miner.* **16**, 262 (1988).
- ⁸²S.C. Kohn, R. Dupree, and M.E. Smith, *Geochim. Cosmochim. Acta* **53**, 2925 (1989).
- ⁸³S.C. Kohn, R. Dupree, M.G. Mortuza, and C.M.B. Henderson, *Am. Mineral.* **76**, 309 (1991).
- ⁸⁴G. Kunath, P. Losso, H. Schneider, S. Steurnagel, and C. Jäger, *Solid State Nucl. Magn. Reson.* **1**, 261 (1992).
- ⁸⁵G. Kunath-Fandrei, T.J. Bastow, J.S. Hall, C. Jäger, and M.E. Smith, *J. Phys. Chem.* **99**, 15138 (1995).
- ⁸⁶G. Paglia, A.L. Rohl, C.E. Buckley, and J.D. Gale, *J. Mater. Chem.* **11**, 3310 (2001).
- ⁸⁷Y. Yourdshahyan, C. Ruberto, M. Halvarsson, L. Bengtsson, V. Langer, and B.I. Lundqvist, *J. Am. Ceram. Soc.* **82**, 1365 (1999).
- ⁸⁸B. Ollivier, R. Retoux, P. Lacorre, D. Massiot, and G. Ferey, *J. Mater. Chem.* **7**, 1049 (1997).
- ⁸⁹B.C. Lippens and J.J. Steggerda, in *Physical and Chemical Aspects of Adsorbents and Catalysts*, edited by B.G. Linsen (Academic Press, New York, 1970), Chap. 4.
- ⁹⁰R.M. Lindstrom, R. Zeisler, and M. Rossbach, *J. Radioanal. Nucl. Chem.* **112**, 321 (1987).
- ⁹¹R.M. Lindstrom, *J. Res. Natl. Inst. Stand. Technol.* **98**, 127 (1993).
- ⁹²R.L. Paul, R.M. Lindstrom, and D.H. Vincent, *J. Radioanal. Nucl. Chem.* **180**, 263 (1994).
- ⁹³P.E. Garret, N. Warr, and S.W. Yates, *J. Res. Natl. Inst. Stand. Technol.* **105**, 141 (2000).
- ⁹⁴G. Paglia, C.E. Buckley, A.L. Rohl, F. Jones, and T. Udovic (unpublished).